

Far infrared mapping of three galactic star forming regions

S.K. Ghosh^{1,2}, B. Mookerjea^{1,3}, T.N. Rengarajan⁴, S.N. Tandon⁵ and R.P. Verma¹

¹Tata Institute of Fundamental Research, Bombay 400005, India

²Institute of Space and Astronautical Science, Kanagawa 299-8510, Japan

³Joint Astronomy Programme, Indian Institute of Science, Bangalore 560 012, India

⁴Department of Physics, Nagoya University, Nagoya 464-8602, Japan

⁵Inter-University Centre for Astronomy & Astrophysics, Pune 411007, India

Abstract. Three Galactic star forming regions in the northern sky, viz., associated with W3(OH), S209 and S187 have been simultaneously mapped in two trans-IRAS far infrared (FIR) bands centered at ~ 140 and $200 \mu\text{m}$ using the TIFR 100 cm balloon borne FIR telescope. These maps show extended FIR emission with structures. The spatial distribution of cold dust ($T < 30 \text{ K}$) for two of these sources (W3(OH) & S209), has been generated from these maps. The HIREs processed IRAS maps of these regions at 12, 25, 60 & $100 \mu\text{m}$ have also been used for comparison. Point-like sources have been extracted from the longest waveband TIFR maps and searched for associations in the other five bands. Their positions, flux densities etc have been determined.

With the aim of mapping with high angular resolution, and at wavelengths beyond the longest waveband of IRAS survey, three star forming regions in our Galaxy, viz., W3(OH), S209 and S187, have been studied. All these three sources are known sites of active star formation of high mass with associated H II regions.

The far infrared (FIR) mapping of W3(OH), S209 and S187 were carried out using the 12 channel two band FIR photometer system ($\lambda_{\text{eff}} \sim 140$ & $200 \mu\text{m}$) at the Cassegrain focus of the TIFR 100 cm ($f/8$) balloon borne telescope (Ghosh 2000). Details of the instruments, observational procedure, image processing and analysis can be found in Ghosh et al. (2000). The achieved angular resolutions in the FIR maps of these three sources are in $1' - 1.5'$ range and the absolute positional accuracy is ~ 0.5 . As an example, the intensity maps in the two TIFR bands for the region around S 209 have been presented in Fig. 1. All the three sources are well resolved in both the bands, some into even multiple components.

The HIREs processed maps (Aumann et al. 1990) from the IRAS survey data (at 12, 25, 60 and $100 \mu\text{m}$) for these three sources have been used for comparison, extracting sources, quantifying interband positional associations and flux densities.

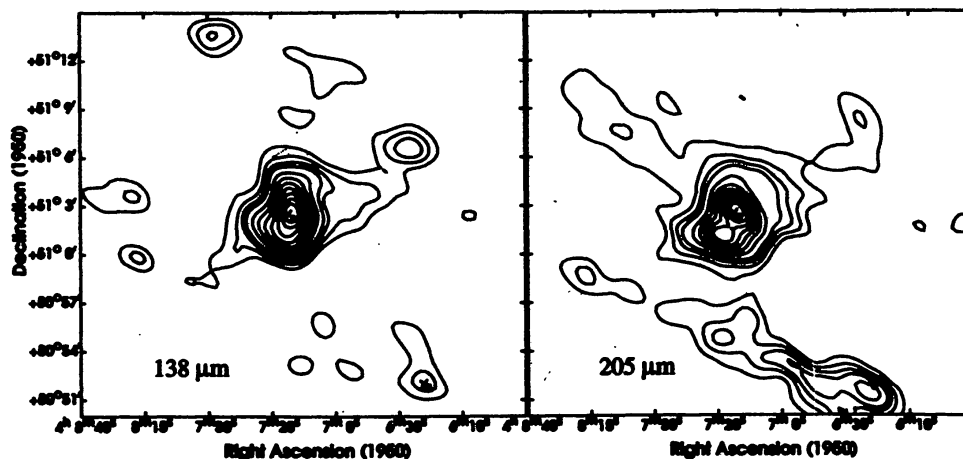


Figure 1. The intensity maps for the region around S29 in TIFR bands - (a) at 138 μm with peak = 441 Jy/sq. arcmin, (b) at 205 μm with peak = 213 Jy/sq. arcmin. The isophot contour levels in both (a) and (b) are 90, 80, 70, 60, 50, 40, 30, 20, 15, 10 & 5% of the respective peaks. The crosses denote the positions of the IRAS PSC sources 04073 + 5102 (main source), 04072+5100 (the nearby source which is resolved in 205 μm map) and 04064 + 5052.

Discrete sources have been extracted from the TIFR and HIREs maps using a procedure described in Ghosh et al. (2000). The longest wavelength channel (TIFR Ch-II) map has been used as the primary band. The sources thus detected in the primary band are associated with sources in other bands if they satisfy the positional match criterion ($<1'$ separation with TIFR Ch-I and $<1.5'$ for HIREs bands). A total of nine sources in all three regions have been detected (six of these have been detected in both the TIFR bands). All these nine sources have an association with HIREs source in at least one band (8 have associations in 2 or more IRAS bands). Flux densities have been obtained in respective bands by integrating over a circle of $3'$ diameter.

Taking advantage of the nearly identical circular beams of the TIFR bands and the simultaneity of observations, reliable maps of dust temperature and optical depth (at 200 μm , τ_{200}) have been generated for W3(OH) and S29 regions. The available dynamic ranges in both the TIFR bands for these two sources allow us to meaningfully determine the dust temperature and optical depth distributions. A dust emissivity law of $\epsilon_{\lambda} \propto \lambda^{-2}$ has been assumed for this purpose. Details of the procedure can be found in Mookerjee et al (2000).

References

- Aumann H.H., Flower J.W., Melnyk M., 1990, AJ 99, 1674
 ghosh S.K., 2000, BASI 28, 225
 Ghosh S.K., Mookerjee B., Rengarajan T.N., Tandon S.N., Verma R.P., 2000, A&A 363, 744
 Mookerjee B., Ghosh S.K., Rengarajan T.N., Tandon S.N., Verma R.P., 2000, AJ 120, 1954